

Quantum Phase and its Measurable Attributes à la Aharonov–Bohm Effect

Sushanta Dattagupta

In this article, we discuss how a combination of electrodynamics and quantum mechanics makes interference measurements of the quantum phase possible in terms of the vector potential, neither of which is detectable independently. This effect, predicted by Aharonov and Bohm, is of great significance in the contemporary interesting topic of nanoscopic physics. We also indicate how the effect can be incorporated in a solid state device by employing the tight-binding (TB) model. The TB model can be realized in a mesoscopic ring which allows the measurement of the bond current and the associated diamagnetism. An exactly solvable case of a three-site ring is presented that serves as a pedagogic example providing further insights into the phenomenon.

1. Introduction

It is almost six decades since Aharonov and Bohm announced an enigmatic effect which is intrinsically of quantum origin [1]. The effect was puzzling enough to evoke disbelief (in the beginning) until decisive experiments laid to rest all the doubts about its veracity [2]. In recent years, mainly because of experimental advances made in the so-called nanoscopic systems, the Aharonov–Bohm effect (ABE, hereafter) has received increased attention [3]. ABE relies on the coherence associated with the quantum phase, and therefore, shares an intimate relation with quantum information processes. Also, since nanoscopic systems are in inevitable and non-negligible interaction with its environment that leads to dissipative effects, the resultant decoherence is challenging to our efforts at protecting quantum information. The implementation of ABE in the laboratory offers device possibilities for



Sushanta Dattagupta, having spent more than forty years in teaching, research and administration in various institutions and universities across India, is now a senior scientist of the Indian National Science Academy. He has written extensively, in journals and books, on topics of condensed matter, non-equilibrium phenomena, and more recently Tagore Model of education. His current physics interests are in quantum dissipation and stochastic thermodynamics of nanoscopic systems.

Keywords

Aharonov–Bohm effect, vector potential, tight-binding model, mesoscopic ring, bond current.



The Aharonov–Bohm effect was puzzling enough to evoke disbelief (in the beginning) until decisive experiments laid to rest all the doubts about its veracity.

systematic studies of the interplay of coherence and decoherence [3].

This article aims to make a simple presentation of the ABE which a student with only rudimentary exposure to electromagnetic theory and elementary quantum mechanics would be able to follow. An exactly solvable model of a mesoscopic ring that can serve as a tutorial in an undergraduate curriculum provides valuable insight into the occurrence of a spontaneous electric current as a consequence of the ABE [4].

With these introductory remarks, the plan of the paper is as follows. In Section 2 we introduce the concept of ABE and the consequent phase changes by juxtaposing electromagnetism with quantum theory. In Section 3, the implementation of ABE is demonstrated in the context of basic solid state physics in terms of what is called the tight-binding model (TB). The resulting analysis allows us to write down expressions for the bond current and concomitant diamagnetism. The exact treatment for a three-site ring is presented in Section 4 [4]. In Section 5, we offer a few summary remarks.

2. What Is Aharonov–Bohm Effect (ABE)?

For a quantum mechanical system, the fundamental quantity that determines all its time-independent properties is the wave function $\psi(\mathbf{x})$ where \mathbf{x} collectively denotes all the coordinates of the system. The simplest example is that of a free quantum particle of momentum \mathbf{p} for which $\psi(\mathbf{x}) = ae^{i\mathbf{p}\cdot\mathbf{x}/\hbar}$, where a is an amplitude which is complex in general, and $\hbar = (h/2\pi)$, h being the Planck constant. The term occurring in the exponent is called the phase $\phi(\mathbf{x}) = \mathbf{p}\cdot\mathbf{x}/\hbar$. However, the absolute phase ϕ is not normally measurable as it drops out from the probability density $|\psi(\mathbf{x})|^2 = |a|^2$ of finding the particle at \mathbf{x} . The situation changes dramatically as we combine quantum mechanics with electromagnetic theory when phase differences can yield interference patterns of electrons, as predicted by Aharonov and Bohm in a fascinating effect named after them [1].

The implementation of the ABE in the laboratory offers device possibilities for systematic studies of the interplay of coherence and decoherence.



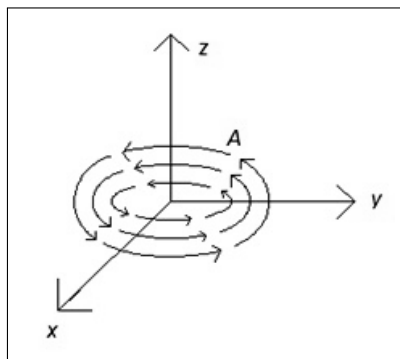


Figure 1. Vortex lines of vector potential because of a magnetic field along the z-axis, in the symmetric gauge.

As we combine quantum mechanics with electromagnetic theory, phase differences can yield interference patterns of electrons.

In electromagnetic theory, Faraday was the earliest proponent of the concept of ‘fields’ in terms of magnetic lines of force [2]. The outcome is what is called a ‘vector potential’ $\mathbf{A}(\mathbf{x})$ that yields the magnetic field \mathbf{B} by the relation $\mathbf{B} = \text{Curl } \mathbf{A}(\mathbf{x})$. (We will consider only the case of uniform \mathbf{B} -field.) Like the quantum phase, the \mathbf{A} -field is not normally a physical attribute as one can add to it $\text{grad } \chi(\mathbf{x})$ (where χ is an arbitrary scalar field) without altering the physical field \mathbf{B} . This property is called the ‘gauge invariance’ of \mathbf{B} . For instance, for a uniform magnetic field applied along the z-direction in the laboratory, one can work with the so-called symmetric gauge in which

$$\mathbf{A} = \left(-\frac{1}{2}yB, \frac{1}{2}xB, 0 \right),$$

which however transforms to the Landau gauge: $\mathbf{A}' = (0, xB, 0)$ when one chooses

$$\chi(\mathbf{x}) = \frac{B}{2}xy.$$

Field lines can influence the quantum phase of an electron even if the latter does not actually intersect the \mathbf{B} -field

Evidently, both \mathbf{A} and \mathbf{A}' would lead to a unique \mathbf{B} . Pictorially, the symmetric gauge can be represented by what is called the ‘vortex flows’, in hydrodynamics (*Figure 1*), whereas the Landau gauge can be represented by the ‘laminar flows’ (*Figure 2*). Thus, radically different field-lines yield the same \mathbf{B} , and as it turns out, can influence the quantum phase of an electron even if the latter does not actually intersect the \mathbf{B} -field, and that is the essence of the ABE.



Figure 2. The vector potential lines (shown by arrows) in Landau gauge.

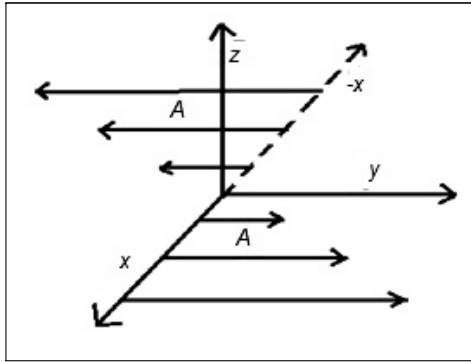
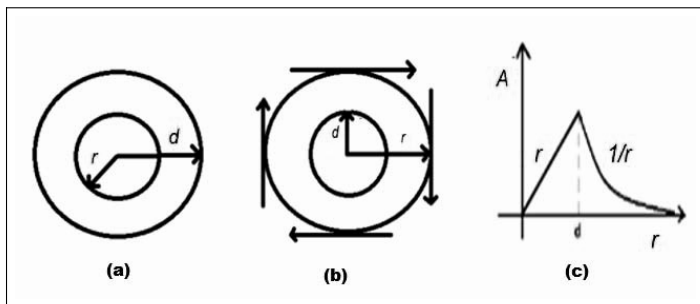


Figure 3. (a) The vortex of $A(r)$ inside. (b) The vortex of $A(r)$ outside. (c) The r -dependence of $A(r)$ inside and outside.



In order to appreciate the effect, we consider the top-down, two-dimensional view of a solenoid that produces a magnetic field going out of the plane of the paper [2]. The \mathbf{A} -field, on the other hand, are vortices, both inside (Figure 3a) and outside (Figure 3b) the coil. If we consider a circle inside the coil of radius r , the Stokes law leads to,

$$B.\pi r^2 = A.2\pi r, \text{ yielding } A = \frac{Br}{2}, \text{ or } A \propto r \text{ (See Figure 3c.)}$$

However, outside the coil of radius d , the \mathbf{A} -field falls off like a Coulomb electrostatic field (Figure 3c):

$$B.\pi d^2 = A.2\pi r, \text{ yielding } A = \frac{Bd^2}{2r}, \text{ or } A \propto \frac{1}{r}.$$

Now imagine a solenoid with vortex \mathbf{A} -fields outside. The \mathbf{A} -fields, however, find themselves in the path of a beam of electrons, emanating from an array of electron sources (Figure 4a). Note that the electron beam does not actually touch the solenoid



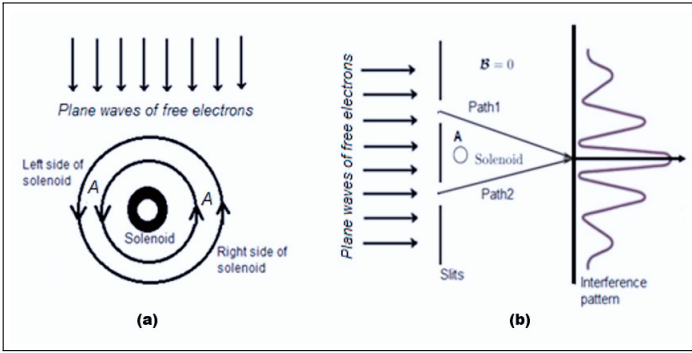


Figure 4. (a) A beam of electrons encountering \mathbf{A} -fields outside the solenoid. (b) Same as in Figure 4a except that the beam is collected in a double-slit geometry by electron bi-prisms on a photographic plate.

but does intersect the vortex lines. Because \mathbf{p} ($= m\mathbf{v}$, without the \mathbf{B} -field) is replaced by $(m\mathbf{v} - e\mathbf{A}/c)$ in electromagnetic theory – the electronic charge being e – the phase $\phi(\mathbf{x})$ becomes $[(m\mathbf{v} - \frac{e\mathbf{A}}{c}) \cdot \frac{\mathbf{x}}{\hbar}]$. Here, \mathbf{v} is the kinematic velocity vector of the electron endowed with mass m . Thus, to the right of the solenoid (Figure 4a), where \mathbf{v} and \mathbf{A} are anti-parallel, there is an increase in the phase while to the left of the solenoid wherein the \mathbf{v} and \mathbf{A} -vectors are parallel, there is a decrease in the phase. Hence, the two ‘right’ and ‘left’ beams acquire a phase difference. Therefore, if they are channelized by two electron bi-prisms and made to combine on a photographic plate (Figure 4b), the resultant phase difference would cause interference patterns of ‘bright’ and ‘dark’ fringes [2]. This is exactly as in the case of interference patterns on a screen of visible light being diffracted through a double-slit. Thus, we find that though the phase and the vector potential are individually non-measurable quantities, in combination with quantum mechanics and electromagnetism, they yield discernible results, thanks to the ABE.

Though the phase and the vector potential are independently non-measurable quantities, in combination with quantum mechanics and electromagnetism, they yield discernible results.

By adding the contribution of the ‘right’ and the ‘left’ beams the net phase change can be written as:

$$\Delta\phi = (e/\hbar c) \int \mathbf{A} \cdot d\mathbf{l} = (e/\hbar c) \iint \mathbf{B} \cdot d\mathbf{S} = (e/\hbar c) \varphi = \varphi/\varphi_0 \quad (1)$$

where $\varphi_0 (= \hbar c/e)$ is the so-called flux quantum. In writing (1) we have again employed the Stokes law which allows a line inte-



gral to be replaced by a surface integral. It is interesting to note that the right-hand side of (1) has no reference to the underlying \mathbf{A} -field, and is, therefore, gauge-independent, as it ought to be, because the left-hand side is a physical quantity.

3. The Tight-binding Model – A Primer

3.1 Zero Magnetic Field Case

The tight-binding (TB) model is an approximate visualization of a periodic crystalline solid in which free atoms are thought to be brought close together and implanted on the lattice sites.

The tight-binding (TB) model is an approximate visualization of a periodic crystalline solid in which free atoms are thought to be brought close together and implanted on the lattice sites. It is natural then that the model reposes on a many-body wave function which is a linear combination of atomic orbitals (LCAO). As free atoms come nearer, the Coulomb interaction between the atom cores and the electrons split the energy levels, spreading them into bands, as discussed below. The TB approximation, though not quite representative of conduction electrons works well for bound electrons such as for the d bands of transition metals and the valence bands of diamond-like and inert gas crystals [5].

Given this background, the TB approximation amounts to the following picture of an electron in a lattice. The electron is more or less localized on the lattice sites barring occasional tunnelling or ‘leaking’ of its wave function to the nearest neighbour sites. We imagine – following a ‘bottom-up’ approach – how the model is built brick-by-brick, in a manner of speaking. Consider what happens when say two hydrogen atoms are brought close together, and their charge distributions are made to overlap. Each hydrogen atom has one electron in the 1s ground state. (In the discussion below we will ignore the more complicated cases of p, d, ... electrons.) The wave functions Ψ_1 and Ψ_2 on the separated atoms 1 and 2 are shown schematically in *Figure 5a* and *5b*. From the Bohr–Rydberg theory, each of these two wave functions is of the form:

$$\psi(\rho) = (1/a_0) \exp(-|\rho|/a_0), \quad (2)$$



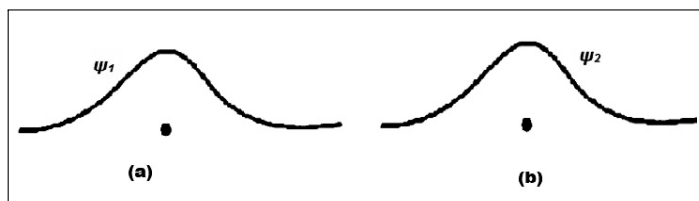


Figure 5. (a) H-like wave function of atom 1. (b) H-like wave function of atom 2.

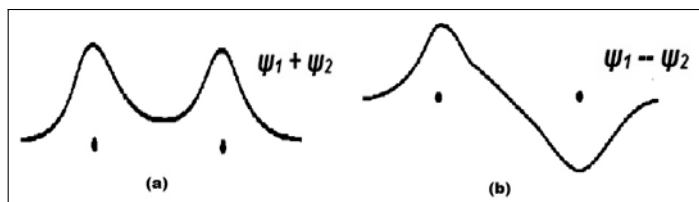


Figure 6. (a) The bonding state. (b) The anti-bonding state.

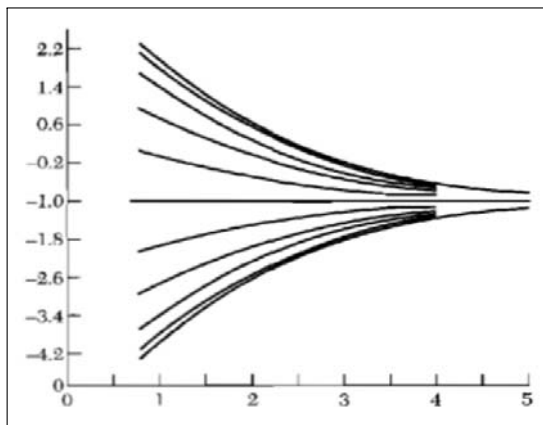
a_0 being the Bohr radius ($= \hbar^2/4\pi m e^2$).

As the atoms come close together and their wave functions overlap, it is no longer sensible to talk about individual (identical) electrons but instead, discuss things in terms of electron density $|\Psi|^2$. The composite system can exist in one or the other of the two possible quantum states which can be formed from the two linear combinations: $\Psi_+ = \Psi_1 + \Psi_2$ and $\Psi_- = \Psi_1 - \Psi_2$, indicated in *Figure 6a* and *6b*. Each combination shares the electrons with two protons. But the electron density in the state $|\Psi_+|^2$ is non-zero in the middle of the two protons thus causing a gain in the attractive Coulomb energy (*Figure 6a*). This is in contrast to the state Ψ_- in which the probability density is zero in the midway region thus being bereft of the benefit of the Coulomb attraction (*Figure 6b*). Therefore, the state Ψ_+ has a higher binding energy than the state Ψ_- . Consequently, Ψ_+ is called the ‘bonding’ state while Ψ_- is called the ‘anti-bonding’ state [6]. As we graduate from 2 to say 20 atoms, 10 orbitals are formed for each pair of degenerate orbitals of two atoms (*Figure 7*). The energy in Rydberg unit is plotted along the ordinate while the nearest neighbour distance (in Bohr radii) is plotted along the abscissa [5].

The preceding remarks make it evident that the TB model has



Figure 7. A band of 10 orbitals for 20 atoms, after C Kittel [5].



The tight-binding model has as its building blocks, a conglomerate of two-state systems – bonding and anti-bonding states.

as its building blocks, a conglomerate of two-state systems – bonding and anti-bonding states. What is the effective Hamiltonian for such a two-state system? To answer this question, it is convenient to ignore the spatial extent of Ψ_1 and Ψ_2 and map them into two Pauli spin states $|+\rangle$ and $|-\rangle$ respectively:

$$\Psi_1 \rightarrow |+\rangle, \Psi_2 \rightarrow |-\rangle . \tag{3}$$

Within this truncated 2×2 Hilbert space, the matrix elements of the underlying Hamiltonian can be written as,

$$\begin{aligned} \langle +|H_{12}|+\rangle &= -\epsilon_+, \langle -|H_{12}|-\rangle = -\epsilon_-, \langle +|H_{12}|-\rangle = -J_+, \\ \langle -|H_{12}|+\rangle &= -J_{-+}, J = J_{+-} = J_{-+}, \end{aligned} \tag{4}$$

where ϵ_+ (ϵ_-) are the site energies and J_{+-} (J_{-+}) are the overlap (or tunnelling) integrals. In a purely symmetric case, of course, the site energies are identical but, in general, they differ because of an omnipresent disorder. Also, note that the states $|+\rangle$ and $|-\rangle$ which refer to two distinct sites are not the eigenstates of the Hamiltonian, while Ψ_+ and Ψ_- are. The negative signs in front of the ϵ 's take care of the attractive interaction leading to 'localized' or TB states. Thus, we can construct the Hamiltonian in terms of Pauli spin matrices as,



$$H_{12} = -\epsilon_0|+\rangle\langle +| + \epsilon\sigma_z + J\sigma_x, \quad \epsilon_0 = (\epsilon_+ + \epsilon_-)/2, \quad \epsilon = (\epsilon_+ - \epsilon_-)/2, \quad (5)$$

Or equivalently,

$$H_{12} = -\epsilon_+|+\rangle\langle +| - \epsilon_-|-\rangle\langle -| - J(|+\rangle\langle -| + |-\rangle\langle +|). \quad (6)$$

The full TB model for the whole crystal is a natural extension of (6) and can be written as,

$$H_{TB} = -\sum_l \epsilon_l |l\rangle\langle l| - J \sum_{\langle lm \rangle} (|l\rangle\langle m| + |m\rangle\langle l|). \quad (7)$$

where $\langle lm \rangle$ implies summation over the nearest neighbour sites. Evidently, the product $|l\rangle\langle l|$ is a projection operator whose expectation value is the probability of finding the electron at the site l . In order to appreciate (see below) how the AB effect is to be incorporated in the TB model, it is useful to rewrite the Dirac bra and kets in terms of their Schrödinger counterparts of wave functions. Thus,

$$\langle r|l \rangle = \Psi(\mathbf{r} - \mathbf{r}_l). \quad (8)$$

3.2 TB Model in the Presence of a Constant Magnetic Field

Having laid the basis of the TB approximation, we now imagine the underlying lattice to be threaded by a vector potential field. As argued in Section 2, the summand in (7) would then be modified by a phase factor $\exp(i\phi_{lm})$ associated with the bond between the sites l and m , and hence, the Hamiltonian becomes,

$$H_{TB} = -\sum_l \epsilon_l |l\rangle\langle l| + J \sum'_{\langle lm \rangle} [\exp(i\phi_{lm}) |l\rangle\langle m| + H.A.], \quad (9)$$

where H. A. abbreviates ‘Hermitian adjoint’. Referring to (1), ϕ_{lm} is given by the total magnetic flux threading the sites l and m .



With this machinery behind us, we calculate what is called the ‘bond current’. To do this we note that the ‘occupation operator’ $n_k = |k \rangle \langle k|$ obeys the equation of motion:

$$\begin{aligned} (d/dt) n_k = (i\hbar) [H_{TB}, n_k] &= (2iJ/\hbar) \sum_l' [\exp(i\phi_{lk}) |l \rangle \langle k| \\ &- \exp(-i\phi_{lk}) |k \rangle \langle l|], \end{aligned} \quad (10)$$

wherein we have worked out the commutator of H_{TB} with n_k : $[H_{TB}, n_k]$, from (9). The prime on l implies that the summation runs only over the nearest neighbour sites of k . Evidently, the left-hand side of (10) is the negative of the operator for the total ‘particle current’ flowing out of the site k , thus

$$I_{kl}(t) = (4J/\hbar) \cdot \text{Im}[\exp(i\phi_{lk}) |l \rangle \langle k|], \quad (11)$$

where ‘Im’ stands for the imaginary component. The ‘electric current’ can be obtained from the particle current in (11) by multiplying it by $-e$, the charge on the electron. In the steady state, the left-hand side of (10) vanishes and hence there is no net current flowing out of the site k , as is expected from the particle (i.e., electron) number conservation. However, between two specific sites there would still be a current as can be detected by inserting an ammeter between the two sites. The latter is sometimes referred to as the ‘bound current’ because it originates from the bounded cyclotron motion of an electron due to the Lorentz force exerted upon it by an external magnetic field. This point is further explained below, in Section 4.

The bond current is related to diamagnetism. An electric current or a flowing charge produces an orbital magnetic moment opposite to the direction of the applied magnetic field.

The bond current is related to diamagnetism. As we know from basic electromagnetism, an electric current or a flowing charge produces an orbital magnetic moment opposite to the direction of the applied magnetic field. This is in contrast to the moment arising from the intrinsic spin of the electron. It is expected, therefore, that the bond current, derived above, would be related to the orbital angular momentum operator whose average yields diamagnetism. In order to establish this connection, we first intro-



duce the basic statistical mechanical definition of the magnetization from the Hamiltonian of a free electron subject to the vector potential \mathbf{A} , given by

$$H_0 = (1/2m) \{ [(p_x + eBy/2c)^2] + [(p_y - eBx/2c)^2] \}, \quad (12)$$

where we have employed the symmetric gauge corresponding to a \mathbf{B} -field along the z-axis. Here p_x and p_y are the x- and y- components of the canonical momentum vector \mathbf{p} . Taking a derivative with respect to B, it is straightforward to see that

$$-(\partial/\partial B) H_0 = (e/2c) (yv_x - xv_y) = (e/2c) (\mathbf{r} \times \mathbf{v})_z = (e/2c) \mu_z, \quad (13)$$

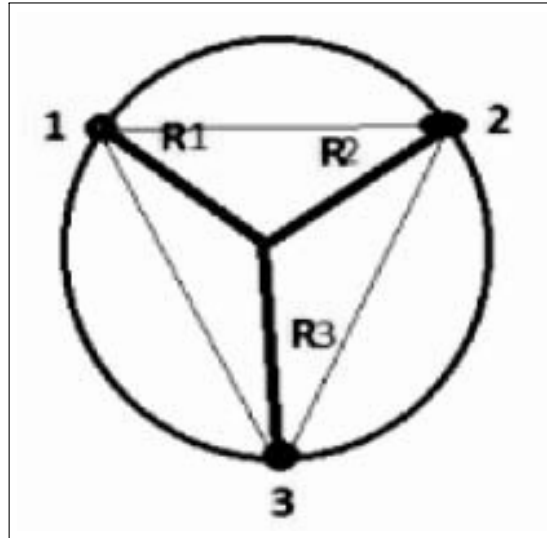
where μ_z is the z-component of the angular momentum operator. The right-hand side is indeed the magnetic moment operator M_z . Using this definition, and the TB form of the Hamiltonian H_{TB} in (9), it is straightforward to ascertain that the average orbital magnetization is given by the expectation value of M_z (denoted by angular brackets, below), calculated with the aid of the canonical partition function [7]. Thus

$$\langle M_z \rangle = -\sum'_{ij} S_{ij} \cdot \langle |_{ij} \rangle . \quad (14)$$

S_{ij} being the area normal to the direction of the magnetic field, comprising the sites i and j which the magnetic flux threads. (14) is a remarkable result in that it relates a thermal equilibrium property such as the average magnetization, derivable from the partition function, to a transport property like the average current, in the steady state. Such a connection is special to the phenomenon of diamagnetism. The analysis here also shows how diamagnetism is linked with the ABE.



Figure 8. A ring with 3 sites labelled as 1, 2 and 3. With the centre as the origin, \mathbf{R} 's are respective radius vectors.



4. A Three-site Ring and Some Exact Results

In this section, we consider a simplified version of the TB model – a mesoscopic ring with just three localized sites. For the ease of calculation, we further assume symmetry among the three sites such that $\epsilon_1 = \epsilon_2 = \epsilon_3 = \epsilon$ and $J_{12} = J_{23} = J_{31} = J$. Further, the triangular geometry automatically ensures that $\phi_{12} = \phi_{23} = \phi_{31} = (e/\hbar c) \mathbf{B} \cdot \mathbf{S}$, where \mathbf{S} is the vector area of the triangle, inscribed by the circle in *Figure 8*, and through which the magnetic flux penetrates. Our objective is to obtain exact results for the bond current and the diamagnetic moment in order to have a clear insight into the ramifications of the ABE [4].

The Hamiltonian in (9) now simplifies to

$$H_{\text{TB}} = J [\exp(-i\phi) (|1\rangle\langle 2| + |2\rangle\langle 3| + |3\rangle\langle 1|) + H.A.], \quad (15)$$

since the first term proportional to ϵ reduces to a constant (because $\sum_l |l\rangle\langle l| = 1$, from closure property) and can be dropped from further considerations. The above has the following 3×3 matrix representation:



$$H_{TB} = J \begin{pmatrix} 0 & \exp(-i\phi) & \exp(i\phi) \\ \exp(i\phi) & 0 & \exp(-i\phi) \\ \exp(-i\phi) & \exp(i\phi) & 0 \end{pmatrix} \quad (16)$$

where the rows and columns are labelled by the sites 1, 2 and 3 respectively (*Figure 8*). The three eigen values are:

$$\begin{aligned} \lambda_1 = 2J \cos \phi, \lambda_2 &= -J(\cos \phi - \sqrt{3} \sin \phi), \lambda_3 \\ &= -J(\cos \phi + \sqrt{3} \sin \phi). \end{aligned} \quad (17)$$

The corresponding eigen functions can be deduced as

$$\begin{aligned} |\Psi_1 \rangle &= (1/\sqrt{3}) \begin{pmatrix} 1 \\ 1 \\ 1 \end{pmatrix}, |\Psi_2 \rangle = (1/2\sqrt{3}) \begin{pmatrix} -1 + i\sqrt{3} \\ -1 - i\sqrt{3} \\ 2 \end{pmatrix}, \\ |\Psi_3 \rangle &= (1/2\sqrt{3}) \begin{pmatrix} -1 - i\sqrt{3} \\ -1 + i\sqrt{3} \\ 2 \end{pmatrix} \end{aligned} \quad (18)$$

Since the particle number is conserved, on the average – in equilibrium – we have from (10) and (11), for $k = 1$,

$$\langle l_{12} \rangle + \langle l_{13} \rangle = \langle l_{12} \rangle - \langle l_{31} \rangle = 0 \quad (19)$$

Similar identities for the sites 2 and 3 imply that (see *Figure 8*)

$$\langle l_{12} \rangle = \langle l_{23} \rangle = \langle l_{31} \rangle. \quad (20)$$

Therefore, it suffices to calculate just one of the currents, say $\langle l_{12} \rangle = \langle l \rangle$ which, from (11) can be read as

$$\langle l \rangle = (4eJ/rm\hbar) \text{Im} [\exp(i\phi) \langle |2\rangle \langle 1| \rangle]. \quad (21)$$



Because the three sites have the following column representation:

$$|1 \rangle = \begin{pmatrix} 1 \\ 0 \\ 0 \end{pmatrix}, \quad |2 \rangle = \begin{pmatrix} 0 \\ 1 \\ 0 \end{pmatrix}, \quad |3 \rangle = \begin{pmatrix} 0 \\ 0 \\ 1 \end{pmatrix}. \quad (22)$$

it is straightforward to see that

$$\langle 1 | \Psi \rangle = (4eJ/\hbar) \cdot \text{Im}[\langle \Psi_1 | 2 \rangle \langle 1 | \Psi_1 \rangle + \langle \Psi_2 | 2 \rangle \langle 1 | \Psi_2 \rangle + \langle \Psi_3 | 2 \rangle \langle 1 | \Psi_3 \rangle] = (4eJ/\hbar) \sin(\phi). \quad (23)$$

The bond current in the stationary state is then a sinusoidal oscillatory current going through maxima and minima and which changes sign as the B-field is reversed since the phase ϕ is odd in B (see (23)). This time reversal property of the current is of course in conformity with one of the fundamental symmetries in physics. Recall that the equation of motion of a free charge such as an electron under the influence of a magnetic field B can be written in terms of the Lorentz force as

$$m(d/dt)\mathbf{v} = -e(\mathbf{v} \times \mathbf{B})/c, \quad (24)$$

and since \mathbf{v} changes sign as the time t is reversed, the only way the equation of motion (24) can remain invariant under time reversal is to flip \mathbf{B} to $-\mathbf{B}$. Since the bond current $\langle l \rangle$ and \mathbf{v} have identical transformation properties under time reversal, changing \mathbf{B} to $-\mathbf{B}$ must be concomitant with a change in sign of $\langle l \rangle$. The oscillatory nature of the bond current – a hallmark of the ABE, has been demonstrated in the laboratory [8].

5. Concluding Remarks

In this paper, we have introduced the Aharonov–Bohm effect and its quantum consequences, in a pedagogical form that ought to be accessible to university students of physics and chemistry. The model is further couched in the much-studied tight-binding model



of the solid state, and a connection is established between the bond current that flows from one site to the other of a lattice and diamagnetism. This connection is elucidated in terms of a ‘symmetric’ three-site mesoscopic ring for which the bond current can be computed exactly.

6. Acknowledgement

I am grateful to Amnon Aharony, Ora Entin–Wohlman and Shmuel Gurvitz for kindling my interest in this topic and valuable suggestions. I thank Tanmay Saha for help in formatting the manuscript. I also acknowledge the support from the Indian National Science Academy through their ‘Senior Scientist’ scheme.

Suggested Reading

- [1] Y Aharonov and D Bohm, Significance of Potentials in Quantum Mechanics, *Physical Review*, Vol.115, p.485, 1959.
- [2] A Tonomura, The Quantum World Unveiled by Electron Waves, *World Scientific*, Singapore, 2000.
- [3] S Dattagupta, Coherence versus Decoherence, *Current Science*, Vol.109, p.1951, 2015. For wider discussions see Y Imry, *Introduction to Mesoscopic Physics*, Oxford University Press, 2nd ed. Oxford, 2002 and S Datta, *Transport in Mesoscopic systems*, Cambridge University Press, Cambridge, UK, 1995.
- [4] The exact results for the 3-site ring are based on notes shared by Amnon Aharony, Ora Entin–Wohlman and Shmuel Gurvitz.
- [5] C Kittel, *Introduction to Solid State Physics*, 6th edition, John Wiley and Sons, New York, N. Y., 1986.
- [6] L Pauling, *The Nature of the Chemical Bond*, Cornell University Press, Ithaca, U.S.A. 1960.
- [7] K Huang, *Statistical Mechanics*, John-Wiley& Sons, New York, 1967; J K Bhattacharjee and D Banerjee, *Intermediate Statistical Mechanics – A Handbook*, World Scientific Press, Singapore, 2017.
- [8] L P Levy, G Dolan, J Dunsmuir and H Bouchiat, *Physical Review Letters*, Vol.64, p.2074, 1990; V Chandrasekhar, R A Webb, M J Brady, M B Ketchen, W J Gallagher and A Kleinsasser, *Physical Review Letters*, Vol.67, p.3578, 1991.

Address for Correspondence
Sushanta Dattagupta
UniworlD City
Heights Tower 6, Flat 002
New Town (Action Area III)
Rajarhat, Kolkata 700 156
Email:sushantad@gmail.com

